Implementation of a passive control system for limiting cavitation around hydrofoils

IOP Conf. Series: Earth and Environmental Science **240** (2019) 032025 doi:10.1088/1755-1315/240/3/032025

Implementation of a passive control system for limiting cavitation around hydrofoils

T Capurso[1], M Lorusso[1], S M Camporeale[1], B Fortunato[1] and M Torresi[1]

[1] Department of Mechanics, Mathematics and Management (DMMM), Polytechnic University of Bari, Via G. Re David, 200 Bari, 70125, Italy

E-mail: tommaso.capurso@poliba.it

Abstract. The performance and the durability of hydraulic systems can be significantly compromised by cavitation. To the aim of delaying cavitation inside turbomachinery, a new passive cavitation control system is proposed in this work. The mentioned system has been applied to a NACA0009 hydrofoil, which accurately reproduces the flow field around real impeller blades. Basically, it consists of slots generating a connection between the suction and the pressure side of the foil. This connection results in a pressure rise close to the leading edge of the foil. Numerical simulations have been performed with the open-source CFD code OpenFOAM and the results have been compared to experimental data available in the literature. The simulations allow to investigate the flow field unsteadiness and the possible flow separation induced by the slots. The passive cavitation control system provides remarkable advantages, i.e., strong reduction of the vapour volume fraction (-93%) accompanied by a reasonable level of loss of performance (lift coefficient reduction equal to -25% and drag coefficient increase equal to +42%). This result is particularly interesting in consideration that the leading edge is only a small part of the entire vane of an impeller.

1. Introduction

In the field of hydraulic turbomachinery (e.g., pumps, turbines, propellers), the occurrence of the cavitation phenomenon can eventually lead to compromise the machine performance and its integrity. Cavitation is the nucleation of vapour bubbles in low pressure regions (below the vapour pressure) and their implosion when the pressure rises again. Depending on the conditions, pressure oscillations are registered with different amplitude and frequency, as revealed by induced noises and vibrations. A region interested by cavitation is called cavity. If the cavity is attached to the machine walls it is said to have a steady behaviour; otherwise, if partially or totally detached and transported downstream, it is said to have an unsteady behaviour. Cavitation can be classified as follows: bubble cavitation, sheet cavitation, cloud cavitation, super-cavitation and vortex cavitation. Each type of cavitation shows specific characteristics, which depend on both fluid properties and operating conditions [1, 2]. Avoiding the occurrence of cavitation can help to preserve the hydraulic turbomachine and to keep high performance. Phenomena which make the study of cavitation complex are, among others: the interaction of phase-changes with turbulence, steep pressure gradients and pressure wave propagation, inducing surface erosion. Many theoretical models, which try to capture the basic cavitation mechanisms, are the result of experiments performed on Venturi ducts [3,4] and hydrofoils [5,6]. Furthermore, in order to

numerically simulate cavitation, different numerical algorithms have been proposed. They can be grouped in the following two approaches [2]: 1) density based compressible solvers with an equilibrium cavitation model; 2) incompressible Navier-Stokes equation solvers for two-phase flows considering the mass transfer among the phases. The latter approach has been often applied in the case of 2D hydrofoils. Each one of the several mass-transfer models available in the literature includes peculiar empirical parameters that must be experimentally tuned for specific geometries and flow conditions [5,6]. Given the significant interaction between turbulence and mass transfer, various combinations of turbulence and mass transfer models have been investigated in order to find the best coupling [7].

To the aim of limiting the cavitation occurrence inside turbomachines and around hydrofoils, either active or passive cavitating flow control techniques have been proposed. An example of active control system is that of ventilation, where gas is intentionally injected by the operator and a cavity is generated around the body to reduce vapour shedding and bubble collapse [8]. On the other hand, passive cavitating flow control systems work autonomously with the purpose of modifying the boundary layer region where cavitation can occur. Among others, trip bars can be cited [9]. In this paper, the proposed cavitation control system belongs to this second class. In consideration of the similarity of the leading edges of the impeller vanes to those of hydrofoils, attention has been focused on the analysis of the cavitation around a two-dimensional hydrofoil, namely a NACA0009, at a fixed angle of attack equal to 2.5°. The results of CFD analyses, carried out using OpenFOAM, have been validated against experimental data provided in the literature by Dupont [10].

The passive cavitation control system here proposed consists of slots, which connect the pressure side to the suction side of the NACA0009 hydrofoil. The numerical investigation has been carried out for a cavitation number $\sigma = ((p_\infty - p_v))/((0.5\rho_\infty U_\infty^2)) = 0.81$ where p_v is the vapour pressure and the subscript ∞ indicates the inlet boundary conditions. Simulations have been run in the OpenFOAM environment by solving the 2D Unsteady Reynolds-Average Navier-Stokes (RANS) equations for incompressible flows according to a finite volume approach (FV). The spatial discretization is performed using a cell centred model. Due to the small angle of attack (2.5°), the investigation described here involves attached cavities, hence making the resolution of the boundary layer phenomena the main concern. Attached cavities are strongly affected by boundary layer behaviour, whereas bubble cavitation is more influenced by pressure gradients and liquid nuclei contents [12]. Moreover, due to the large variation of the Reynolds number when the pressure falls below the vapour pressure, the k-kl-ω model [13, 14] has been preferred, due to its ability to correctly predict the pressure distribution over the suction side of the hydrofoil under laminar-to-turbulent boundary layer transition, as shown by Capurso et al. [7]. The NACA0009 performance (although in the described modified version) has been evaluated in terms of vapour volume fractions and force coefficients. Despite inducing a performance degradation (25% reduction of lift coefficient and 42% increase of drag coefficient), the passive cavitation control system shows a significant reduction of the vapour volume fraction (-93%).

2. Governing equations

To the aim of investigating through numerical modelling in OpenFOAM the phenomena described so far, the interPhaseChangeFoam solver has been selected to solve 2D U-RANS equations and reproduce quasi-steady sheet cavitation and likely flow unsteadiness due to the introduction of slots as passive cavitation control system on the NACA0009 hydrofoil. This solver has been developed for 2 incompressible, isothermal, immiscible fluids including the phase-change. It uses a volume of fluid (VoF) phase-fraction based interface capturing approach. The momentum and other fluid properties refer to the mixture and a single momentum equation is solved. The set of phase-change models provided is designed to simulate cavitation; nonetheless,

other phase-change mechanisms are supported within this solver framework. Indeed, the solver allows to deal with different time and scale of turbulence (DNS, LES or RANS) and to select various turbulence models. The equations of momentum (1), continuity (2) and mass transport (3) are defined as follows:

$$\frac{\partial \rho_m u_i}{\partial t} + \frac{\partial (\rho_m u_j u_i)}{\partial x_j} = -\frac{\partial p}{\partial x_j} + \frac{\partial}{\partial x_j}\left[\mu_m \left(\frac{\partial u_i}{\partial x_j} + \frac{\partial u_j}{\partial x_i}\right) - \mu_m \frac{2}{3}\frac{\partial u_k}{\partial x_k}\delta_{ij}\right] \tag{1}$$

$$\frac{\partial \rho_m}{\partial t} + \frac{\partial (\rho_m u_j)}{\partial x_j} = 0 \tag{2}$$

$$\frac{\partial (\rho_l \alpha_l)}{\partial t} + \frac{\partial (\rho_l \alpha_l u_j)}{\partial x_j} = \dot{m}^+ + \dot{m}^- \tag{3}$$

$$\rho_m = \rho_l \alpha_l + \rho_v \alpha_v \tag{4}$$

$$\mu_m = \mu_l \alpha_l + \mu_v \alpha_v \tag{5}$$

The three phases (liquid, vapour and mixture) are distinguished through the subscripts (l, v, m), respectively, whereas the subscripts (i, j, k) denote the directions of the Cartesian coordinate system. On the right side of eq. (3) the source, $(\dot{m}^+)$, and the sink term, $(\dot{m}^-)$, represent the phase change phenomenon in terms of condensation and evaporation rates. The interPhaseChangeFoam solver includes three mass transfer models, namely: Schnerr and Sauer [11], Kunz [15] and Merkle [16]. Among the three mass transfer models provided by the solver, for this specific application and flow operating conditions the Schnerr and Sauer model has been chosen. Its source terms are defined as follows:

$$\dot{m}^- = 3C_v \rho_v \rho_l \sqrt{\frac{2}{3\rho_l}} \frac{1}{R\rho_m \sqrt{|p - p_v|}} (1 - \alpha_m + \alpha_l) min(p - p_v, 0) \tag{6}$$

$$\dot{m}^+ = 3C_c \rho_v \rho_l \sqrt{\frac{2}{3\rho_l}} \frac{1}{R\rho_m \sqrt{|p - p_v|}} \alpha_l max(p - p_v, 0) \tag{7}$$

and they are based on the Rayleigh-Plesset equation. This model considers a uniform and homogeneous distribution of vapour nuclei dispersed inside the flow, whose presence and location, under specific flow conditions, is responsible for the development of cavitation. The vapour nuclei properties are numerically defined when 2 parameters are known, i.e., the amount of nuclei (n) and their diameters (d_{nuc}). These flow features are usually identified by means of water quality tests in laboratory. In the literature, the influence of these parameters on the simulation results has been often investigated [17]. As a consequence, using data provided by previous studies [17], the value of n and d_{nuc} have been set equal to $1 \cdot 10^{13}$ and $2 \cdot 10^{-6}$ m respectively, and the condensation (C_c) and evaporation (C_v) coefficients equal to 1. These mass transfer model equations have been solved in combination with either k-ω SST or k-kl-ω models for turbulence closure [7,13,14,19]. All the simulations run in this work assume a Courant number roughly equal to 0.3. In order to guarantee stability and accuracy of the simulations, the equation terms have been computed as follows: the gradient terms using a second-order upwind scheme and a cell limited scheme for the pressure, the convection terms using a second-order backward scheme, the turbulence terms using a first-order upwind scheme, the laplacian terms using a limited corrected scheme, while the time integration scheme is a first-order Euler scheme.

3. Numerical domain and boundary conditions

The 2D numerical domain (Figure 1) has been drawn with the aim to reproduce the main dimensions of the Cavitation Research Facility at EPFL, Lausanne [10]. In particular, the foil has been placed at mid height of the channel and the length of the channel along the flow direction is $3.5c$ upstream and $5.5c$ downstream of the foil ($c = 100\ mm$) to reduce the influence of the applied boundary conditions nearby the hydrofoil.

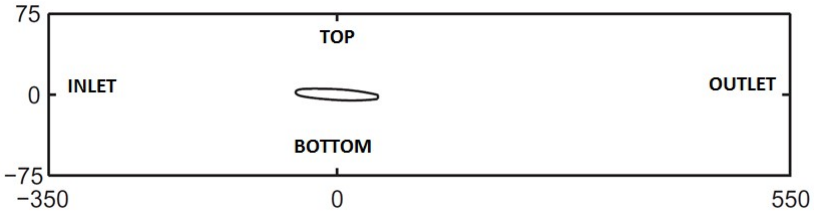

Figure 1. Representation of the numerical domain, dimensions in mm.

The hydrofoil is a modified NACA0009, with maximum thickness at 50% of the initial chord (100 mm). Moreover, its geometry is modified with the purpose to obtain a trailing edge height equal to 3.22 mm where it is truncated, at 90% length, see Figure 2 [10,18]. The boundary conditions applied to the domain are: uniform velocity at the inlet, U, equal to 20.7 m/s, with constant turbulent intensity equal to 1%; uniform pressure at the outlet to achieve a cavitation number $\sigma = (p_\infty - p_v)/(0.5\rho_\infty U_\infty^2) = 0.81$, where p_∞ is the pressure measured at 250 mm upstream of the foil. On the walls, the hydrofoil surfaces and the top and bottom of the channel, a no-slip boundary condition is applied. The properties of the fluid in the experimental set up are $\rho = 998.7\ kg/m^3$ and $\nu = 1.08 \cdot 10^{-6}\ m^2/s$, which corresponds to pure water at 17 °C. The vapour pressure of the water at 17 °C is $p_v = 1938.4\ Pa$ and the vapour density and kinematic viscosity are $\rho = 0.014493\ kg/m^3$ and $\nu = 6.66 \cdot 10^{-4}\ m^2/s$, respectively [10]. The grids have been generated by means of the commercial code Pointwise Gridgen®. They have been converted in a compatible OpenFOAM format and then checked with the command checkMesh to evaluate the quality of the mesh in terms of aspect ratio (<1000), skewness (<0.98) and non-orthogonal cells (< 70°). Three different meshes (fine, medium and coarse) have been generated and simulations of the foil under steady-state fully wetted (non-cavitating) conditions have been run to perform a grid sensitivity analysis. The region in the vicinity of the hydrofoil has been discretized with unstructured triangular elements, whereas the three grids differ for the eight of the first prism layer close to the wall and the grid refinement close to the leading and trailing edge. The total number of cells is 114 000, 48 000 and 31 000 cells, for the fine, medium and coarse mesh respectively. The grid details are shown in Figure 2 and the value of the $y^+ = yU_\tau/\nu$, where y is the first cell height, and U_τ is the wall frictional velocity, are reported in Table 1. Furthermore, in Table 1 the values of the force coefficients calculated at the end of the simulations through the k-ω SST turbulence model are summarized and compared with the experimental data provided by Dupont [10].

Finally, the fine mesh (114 000 cells) has been chosen for further multi-phase simulations, as marginal deviations are found between the three grids, but the finer one presents a better grid resolution close to the leading edge and y^+ value lower than 1. In Section 5 the results of multi-phase simulations on the NACA0009 hydrofoil at a fixed angle of attack, $\alpha = 2.5°$, under steady flow conditions for the quasi-steady sheet cavitating case ($\sigma = 0.81$ and $Re = 2 \cdot 10^6$) are shown.

Table 1. Results of the grid sensitivity analysis. Comparison of the force coefficients, calculated for three grids, and the experimental data [10].

	$n.cells$	$C_D = \frac{D}{1/2\rho U^2 c}$	$C_L = \frac{L}{1/2\rho U^2 c}$	$err.C_D$	$err.C_L$
Dupont P. (experimental)		0.0214	0.315		
Coarse mesh (y^+=70)	31000	0.0221	0.355	-3.3%	-12.7%
Medium mesh (y^+=30)	48000	0.0237	0.355	-10.7%	-12.7%
Fine mesh (y^+=1)	114000	0.0208	0.362	2.8%	-14.9%

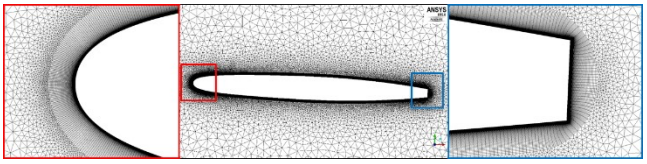

Figure 2. Mesh details.

4. Passive control system

The new passive cavitation control system, to be applied to the NACA0009 hydrofoil, consists of slots creating a connection between the pressure and the suction side of the foil, which allows the flow to pass through the foil, as displayed in Figure 3, and to transport pressure information from one side to the other. The connection is realized by means of three slots (Figure 3), which are designed to suppress the cavity occurring on the suction side of the foil. Both the distance of the first slot from the leading edge and the spacing between the slots are equal to 5% of the chord. The slots are characterized by variable section, i.e., it increases from the pressure to the suction side, and their inclination to the chord is 30°. This geometry allows the flow to decelerate, thus avoiding flow separation at their exits. Indeed, the portion of the main flow which comes up the slots is forced to adhere to the suction side of the foil because it is pushed towards the trailing edge by the main flow. This configuration can be used to reduce cavitation at different angles of attack, so it can be simulated to reproduce the blades of centrifugal pumps at part-load. Since there is no symmetry with respect to the chord of the foil, this modification can work only either at part or at over loads. The study of a symmetric configuration, to be preferred when the machine works both at part and over loads, is on-going. The 2D numerical domain described for the regular foil has been then modified to implement the passive control system; unstructured elements with prism elements close to the foil and inside the slots have been used, imposing the same height for the first cell as that on the suction and the pressure side.

5. Results and Discussion

Unsteady simulations have been run under cavitating flow conditions. The time step has been calculated as a fraction of the characteristic time of the flow $\Delta t = 5.0 \cdot 10^{-6} s = t_\infty/1000 = (c/U_\infty)/1000$. The total duration of the simulation has been set equal to 0.3 s (60 passages of the flow over the foil). The results are shown as average values over a time interval corresponding to the last 20 passages of the flow ($20t_\infty$).

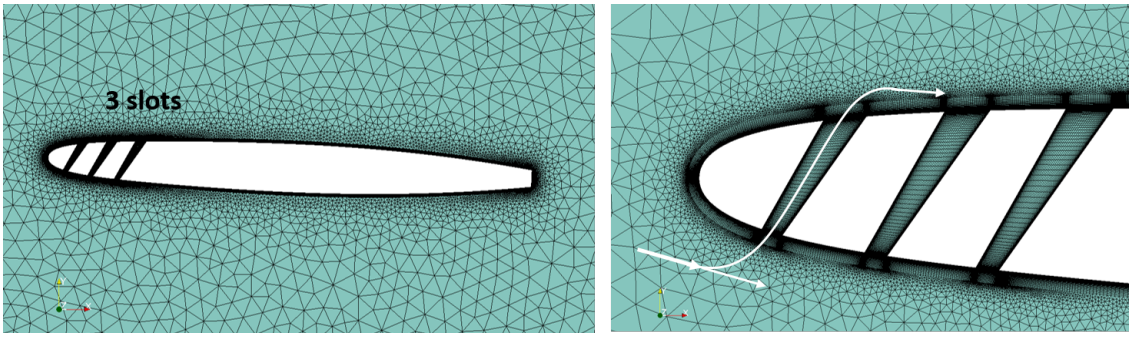

Figure 3. Details of the three slots and their discretization. In white arrows, a representation of the flow passing through the slots.

5.1. Single-phase flow simulations

Firstly, the regular and the modified geometry have been investigated with the solver pimpleFOAM. The pressure coefficient (C_p) for the two geometries has been calculated and compared in Figure 4 to that obtained experimentally by Dupont [10]. As can be seen from Figure 4, the passive cavitation control system influences the pressure distribution on the foil up to 30% length starting from its leading edge. In particular, the pressure is seen to rise on the suction side, generating a consequent decrease of the $-C_p$. This causes a reduction of the performance in terms of force coefficients (lift and drag) as shown in Table 2.

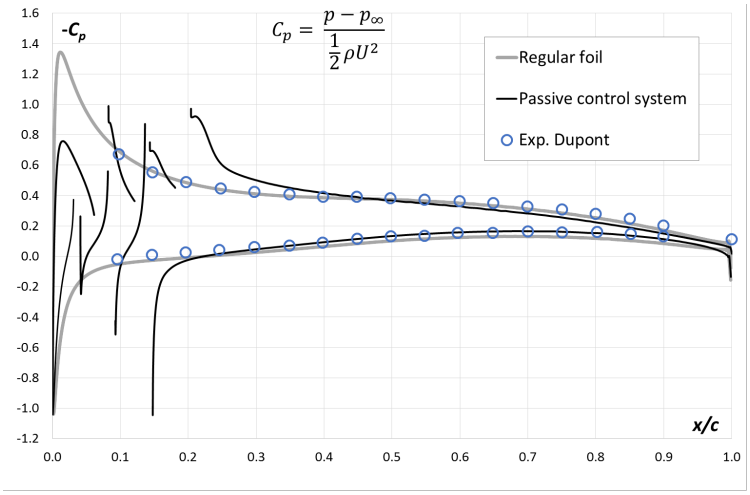

Figure 4. Comparison of the pressure coefficient measured experimentally [10] and calculated via numerical simulations (NACA0009 hydrofoil with $\alpha = 2.5°$ in fully wetted flow condition with k-ω SST [19] turbulence model).

The introduction of the slots also modifies the velocity field downstream their exit on the suction side, see Figure 5. Remarkably, a higher boundary layer close to the suction side of the foil and a reduction of the viscous stress on the suction side of the foil are obtained. Due to the specific geometry of the slots, a recirculation zone is developed inside the slots which decelerates the flow exiting the slots and simultaneously transmits pressure information from the pressure to the suction side (Figure 6).

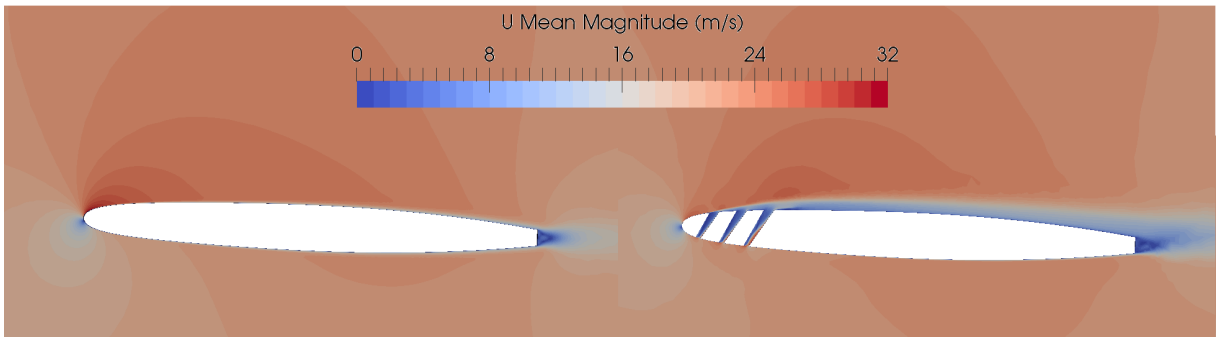

Figure 5. Contours of the mean velocity around the regular and the modified foil.

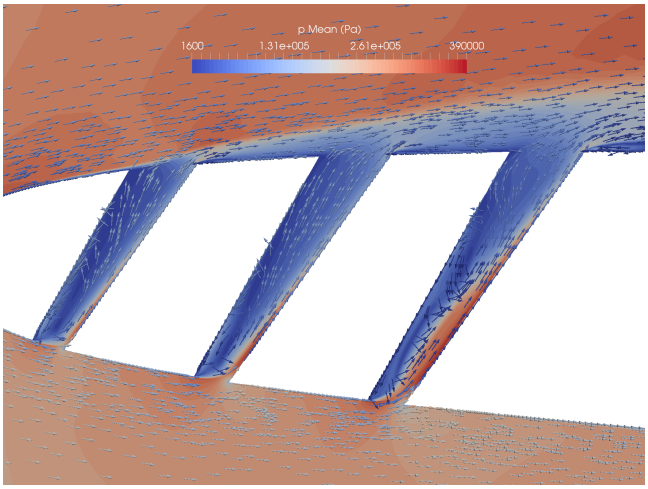

Figure 6. Velocity vectors colored by mean pressure on the contours of the mean velocity inside the slots.

Table 2. Comparison of the hydrofoil performance (lift and drag coefficient) under fully wetted condition with and without the passive control system.

	C_D	C_L
Regular foil	0.0253	0.364
Passive control	0.0355	0.272
Difference %	+42%	-25%

5.2. Multi-phase flow simulations

The multi-phase simulations have been run by employing the mass transfer model proposed by Schnerr and Sauer [11] in combination with the k-kl-ω turbulence model [7,13,14]. Figure 7 compares the pressure coefficients of the regular foil to the experimental data collected by Dupont [10]. The two curves appear to be in good agreement. Also the pressure coefficient of the modified geometry presents a similar trend and keeps the same shape, either under wetted and cavitating flow conditions. Thus, the passive cavitation control provides the same pressure rise on the suction side (Figures 4, 5).

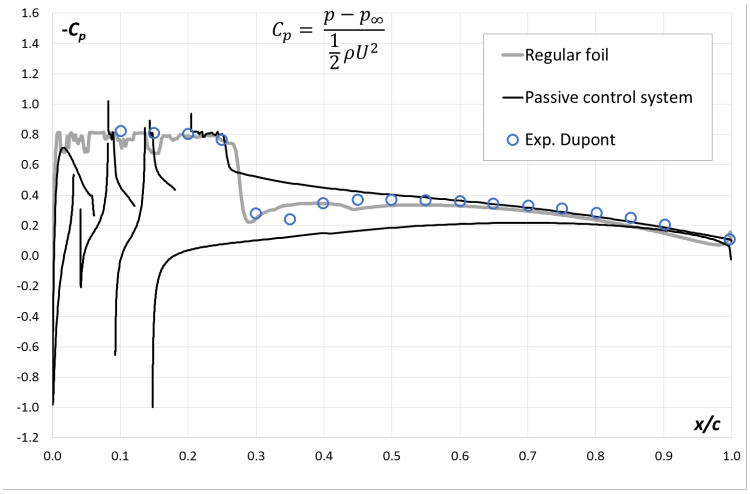

Figure 7. Comparison of the pressure coefficient measured experimentally [10] and calculated via numerical simulations (NACA0009 hydrofoil with $\alpha = 2.5°$, mass transfer model proposed by Schnerr and Sauer [11] and k-kl-ω turbulence model.

To investigate the presence of flow separation, the velocity around the leading edge of the foil has been explored. Differently from the regular foil, which shows recirculation inside the cavity, the flow passing through the ducts in the modified geometry does not undergo any separation at the exit of the channels, except around the corners, see Figure 8.

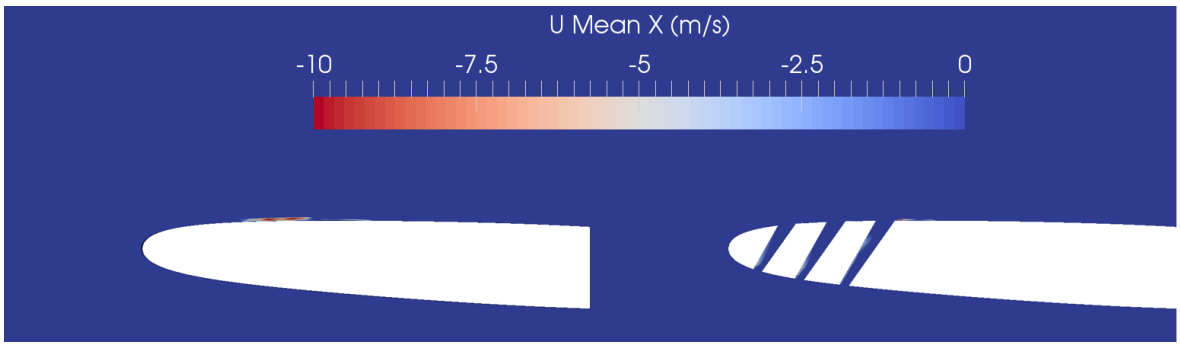

Figure 8. Contours of the velocity x component mean ($UMean\ X$) in order to highlight regions affected by flow separation.

If water volume fraction α_w is considered (Figure 9), the passive cavitation control system is seen to be able to suppress the cavity by 93% (Table 3) by increasing the pressure on the suction side close to the leading edge. The system works autonomously, as wished, producing the effect shown in Figure 9 and 10.

6. Conclusions

A new passive cavitation control system has been proposed with the aim to reduce the cavity occurring on the suction side of an hydrofoil under incipient cavitation conditions. The system consists of slots with a specific geometry, which connect the pressure to the suction side of the foil. The system has been applied to a NACA0009, for which results of experimental tests

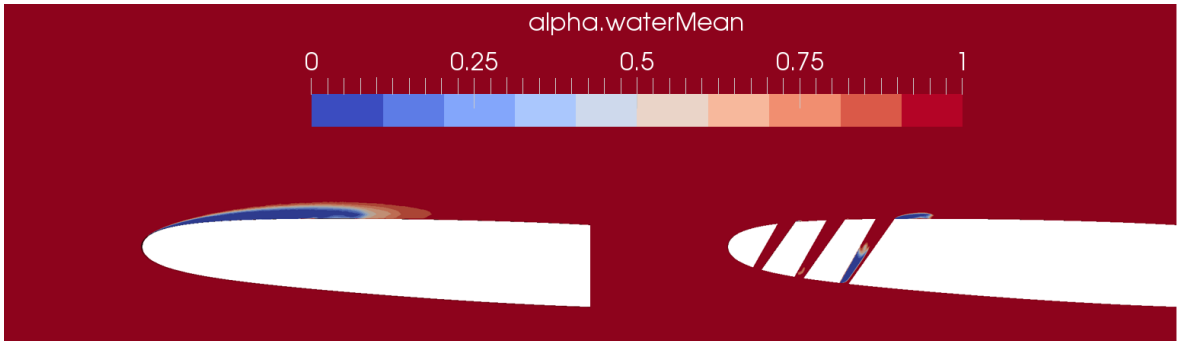

Figure 9. Contours of the mean alpha water fraction, with and without the introduction of the passive cavitation control.

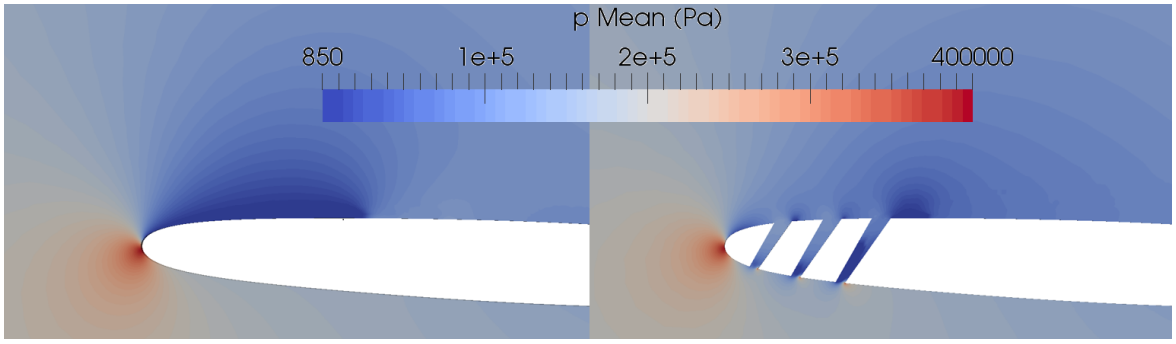

Figure 10. Contours of the mean static pressure, with and without the introduction of the passive cavitation control.

Table 3. Comparison of the cavitation number (σ) and alpha water volume fraction (α_{vapour}) in cavitating flow condition with and without the passive control system.

	σ	α_v
Regular foil	0.810	2.65E-08
Passive control	0.815	1.85E-09
Difference %	+0.6%	-93%

are available in the literature. Numerical simulations have been run under fully wetted and, then, under cavitating flow conditions in order to evaluate the modified geometry behaviour against that of the regular one. 2D U-RANS simulations have been run with the k-ω SST under wetted condition and the k-kl-ω model for multiphase flows for turbulence closure. The performance of the two geometries with non-cavitating flow allowed to investigate the fluid flow inside the slots and to verify the absence of flow separation at their outlets. Moreover, this analysis pointed out the performance reduction of the modified geometry in terms of lift and drag coefficients. Nevertheless, when cavitating conditions are applied, the modified hydrofoil induces a large reduction of the vapour cavity (-93%). However, this result brings about a performance reduction (C_L -25%, C_D +42%) which is not negligible considering how short the length of the foil is. If the system is applied to a real pump impeller, in which the losses are

localized in the initial part of the vanes, a strong reduction of the cavity may be generated, thus improving the functionality of the impeller and enlarging its operating range. In the future, a set of simulations is intended to verify the ability of the passive control system to control and reduce the cavitation inception at different angles of attack by covering different pump operating conditions.

References

[1] Brennen C E 1995 *Cavitation and Bubble Dynamics* (Oxford University Press)
[2] Brennen C E 1995 *Fundamentals of Multiphase Flows* (Oxford University Press)
[3] Barre S, Rolland J, Boitel G, Goncalves E and Fortes Patella R 2009 Experiments and modeling of cavitating flows in venturi: attached sheet cavitation *European Journal of Mechanics B/Fluids* **28** 3 pp 444-464
[4] Stutz B and Reboud JL 1997 Experiments one unsteady cavitation. *Exp. Fluids* **22** 3 pp 191-198
[5] Cervone A, Bramanti C, Rapposelli E and dAgostino L 2006 Thermal cavitation experiments on a NACA 0015 hydrofoil *J. Fluids Eng.* **128** 2 pp 326-331
[6] Dular M, Bachert R, Stoffel B and irok B 2004 Experimental evaluation of numerical simulation of cavitating flow around hydrofoil *European Journal of Mechanics B/Fluids* **24** 4 pp 522-538
[7] Capurso T, Lopez M, Lorusso M, Torresi M, Pascazio G, Camporeale S M and Fortunato B 2017 Numerical investigation of cavitation on a NACA0015 hydrofoil by means of OpenFOAM *Energy Procedia* **126** pp 794-801, ISSN 1876-6102
[8] Kumagai I 2015 Power-saving device for air bubble generation using a hydrofoil to reduce ship drag: Theory, experiments, and application to ships *Ocean Engineering* **95** pp 183-194
[9] Huang J 2017 Passive control of cavitating flow around an axisymmetric projectile by using a trip bar *Theoretical and Applied Mechanics letters* **7** 4 pp 181-184
[10] Dupont P 1991 Etude de la dynamique dune poche de cavitation partielle en vuede la prediction de lerosion dans les turbomachines hydrauliques Ph.D. thesis Ecole Polythechnique Federale de Lausanne, Lausanne, Switzerland
[11] Sauer J and Schnerr G H 2000 Unsteady cavitating flow - a new cavitation model based on a modified front capturing method and bubble dynamics *In Fluids Engineering Summer Conference Proceedings of FEDSM*
[12] Michel J M and Franc J P 2004 *Fundamentals of Cavitation*
[13] Walters K and Cokljat D 2008 A Three-Equation Eddy-Viscosity Model for Reynolds-Averaged NavierStokes Simulations of Transitional Flow *J. Fluids Eng* **130** 12
[14] Furst J 2013 Numerical simulation of transitional flows with laminar kinetic energy *Engineering Mechanics***20** 5 pp 379-388
[15] Kunz R F, Boger D A, Stinebring D R, Chyczewski T S, Lindau J W, Gibeling H J, Venkateswaran S and Govindan T R 2000 A preconditioned Navier-Stokes method for two-phase flows with application to cavitation prediction *Computers & Fluids* **29** 8 pp 849-875
[16] Merkle C L, Feng J Z, and Buelow P E O 1998 Computational modeling of the dynamics of sheet cavitation *Proc. Proceedings of the 3rd International Symposium on Cavitation*
[17] Asnaghi A, Feymark A and Bensow R E 2015 Numerical simulation of cavitating flows using OpenFOAM *18th Numerical Towing Tank Symposium.*
[18] Bouziad Y A 2005 Phisical modelling of leading edge cavitation: computational methodologies and application to hydraulic machinery Ph.D. thesis Ecole Polytechnique Federale de Lausanne
[19] Menter F R 1994 Two-Equation Eddy-Viscosity Turbulence Models for Engineering Applications *AIAA Journal* **32** 8 pp. 1598-1605.